

Extended Abstract for the Minisymposium
The 11th International Conference
on Fracture Turin, Italy, 20-25 March, 2005,

Multi-scale fracture via tectonofractographic and electromagnetic radiation techniques

Dov Bahat

Dept. Geological and Environmental Sciences, Ben Gurion University of the Negev, Beer Sheva , Israel

Introduction

This study uses fractography, tectonofractography and electromagnetic radiation techniques in order to show that generally, the “fundamental laws governing the evolution of fracture remain unchanged across various scale levels, from microscopic to global, i.e. associated with natural processes occurring in the earth crust”, which is the philosophy of this symposium. While arbitrary loading on a structure could often result in a mixed mode loading, a growing crack quickly goes through a mode adjustment and turns so as to reorient itself into mode I fracture¹. Hence, mode I fracture dominates fracturing in various scales, as exemplified below. **The basics** of these techniques are briefly outlined and then, several examples are presented.

Fractography is the common term used in describing the morphology of fracture surfaces. There are conventionally some ten basic features that characterize idealistically a fracture surface (**Figs. 1a-d**). In practice however, only several of these features occur on a single surface and the researcher often needs to complete the picture by comparing a few related fractographies. Fractography. is an important multidisciplinary tool. This tool provides the information on the location of fracture initiation, mode of fracture propagation and causes and mechanism of the failure process. It has been used by investigators of fracture in various synthetic brittle, quasi brittle and non-brittle materials. Just to mention a few examples, the list includes: Experts of glass^{2,3} (e. g. Preston 1926; Sharon and Fineberg 1999), ceramic articles^{4,5} (**Kirchner and Gruver 1973; Mecholsky et al. 1976**), non-silicate

glasses such as bitumene⁶ (De Freminville 1914), vitreous carbon⁷ (Nadeau 1974), polymethylmethacrylate^{8,9,3} (Wolock et al. 1959;; Doll 1975////) polymerized transparent resin¹⁰ (Shinkai and Sakata 1978), steel¹¹ (Irwin 1962) and chromium¹² (Bullen et al. 1970), germanium single crystals¹³ (Haneman and Pugh 1963), jellies¹⁴ (Preston 1931), cellulose acetate¹⁵ (Kies et al. 1950) and rubber¹⁶ (Bhowmick 1986). Fractography was also applied to minerals like quartz^{17,18} (Payne and Ball 1976; Hamil and Sriruang 1976) and sapphire¹⁹ (Congleton and Petch 1967).

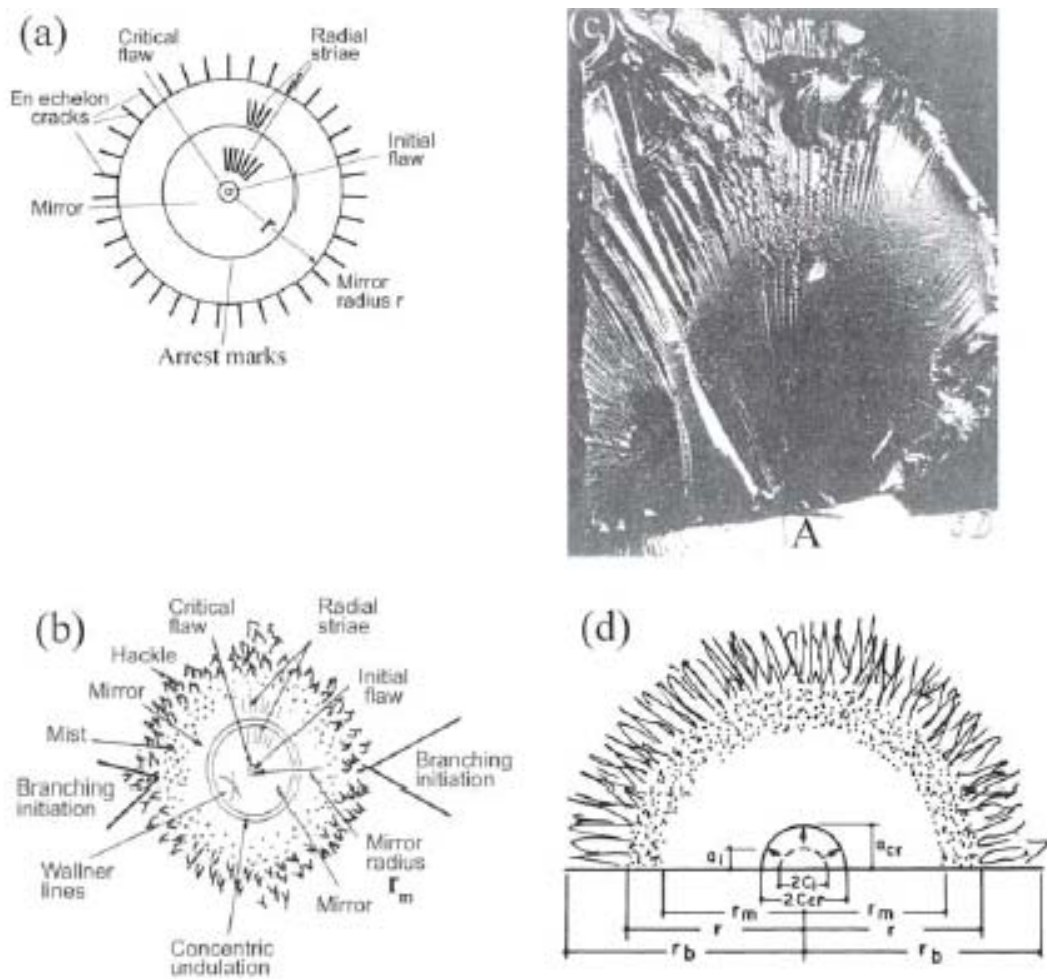


Fig. 1a-d Schematic representation of various fractographic elements on a fracture surface and distinguishing the mirror from the fringe. **a** The mirror radius, r (arrow) is measured from the critical flaw to the inner boundary of the *en echelon* fringe. **b** The mirror radius, r_m (arrow) is measured from the critical flaw to the inner boundary of the mist. Branching may initiate either from the outer rim of hackles at the right or from the inner rim of hackles, at the left (forming hackle and branching initiation together). **c** A fracture

surface in bitumene (from De Freminville 1914). Note a few radial striae within the mirror plane and a multitude of hackles beyond it. Many hackles appear as echelon cracks, extensions of the striae. **d** Schematic fracture surface of brittle materials showing idealized initial flaw length $2c_{ci}$ and depth a_i , critical flaw length $2c_{cr}$ and depth a_{cr} . The three mirror radii, r_m (mirror-mist boundary) r (mist-hackle boundary) and r_b (initiation of microscopic crack branching) are shown as well (modified from Mecholsky and Freiman 1979)

Tectonofractography, which is a derivative of fractography has become a basic instrument in the interpretation of failure in geological structures which are far larger than those examined in the laboratory²⁰ (Bahat 1991). Although the basic morphological features that characterize the fracture surface are known for more than hundred years^{21,6} (Woodworth 1896; De Freminville 1914), there is still a debate on their terminology and on their real significance^{20 (p. 18)} (Bahat 1991, p.18). Fortunately, recent experimental results combined with fresh observations from geological exposures help to resolve these outstanding difficulties and provide a sound basis for a more sophisticated interpretation of failure phenomena in the future²² (Bahat et al. 2004). The correct qualitative terminology and interpretation of the characteristic features described in Figs. 1a and 1b is important for their quantitative applications. These applications relate to the estimation of fracture-stress in fractography and to the estimation of paleo-fracture-stress in tectonofractography (see below). It is also essential for plotting the fractographic data on stress intensity versus fracture velocity curves (Figs. 1d and 2).

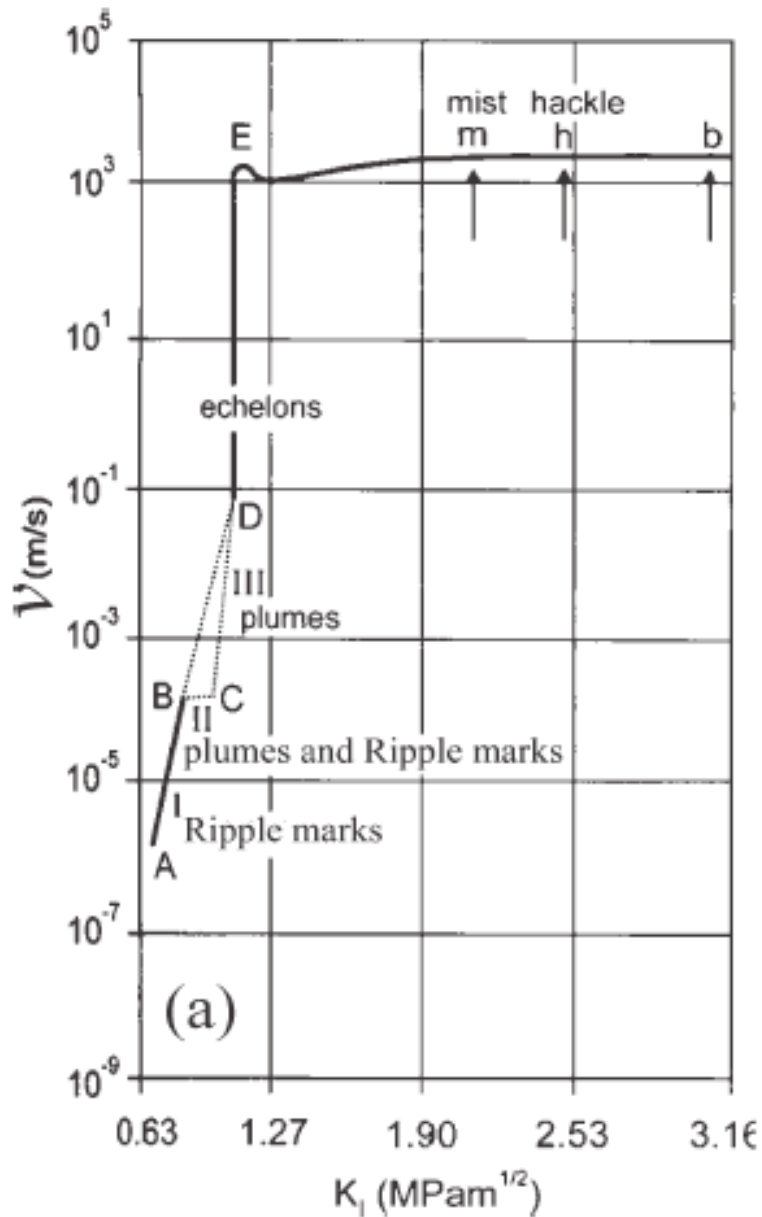


Fig. 2a The V vs. K_I curve for joints in granite from the South Bohemian Pluton, synthesized from laboratory experiments. **b** The estimate of a range of crack velocities for ten joints in granite from the South Bohemian Pluton. For each joint the range of fracture velocity is given in a *rectangular frame* constructed on the curve from Fig. 4.35a, where the vertical right side of each frame gives the maximum fracture velocity that was attained by the joint

Electromagnetic radiation techniques

The fracture of material induces the emission of electrons and positive ions, neutral

atoms and molecules, visible photons and radio waves. We concentrate on electromagnetic radiation in the frequency range 10 kHz–50MHz (denoted here by EMR). EMR from materials fractured under compression was first observed by Stepanov²³ in 1933 for samples of sylvine KCl²⁴ (Urusovskaja 1969). This investigation was followed by numerous others, which measured EMR from a very wide range of piezo and nonpiezoelectric, crystalline and amorphous, metallic and nonmetallic materials and rocks under different stress loadings²⁵⁻²⁷ (O’Keefe and Thiel 1995, Ueda and Al-Damegh 1999, Yoshida 2001). Following these investigations, the interest in fracture emitted EMR shifted from the basic nature of the phenomenon to a more applied nature connected to problems of earthquake prognosis²⁸⁻³⁰ (Warwick *et al* 1982; Ueda and Al-Damegh 1999, Yoshida 2001), the forecast of rock failure in underground mines³¹⁻³³ (Khatiashvili 1984, Frid 1997; Vozoff and Frid 2001) and the study of explosions³⁴⁻³⁵ (Sakai *et al* 1992 Rabinovitch *et al* 2002a). Previous attempts to explain the origin of EMR from fracture were unable to explain all the features of the detected radiation³⁶⁻³⁸ (King 1983, Rabinovitch *et al* 1995, Freund 2002). Based on experimental investigations conducted in our laboratory and other supporting evidence we present a new model, that seems to fit all existing data³⁹. Vladimirov *et al* 2003

Fracture in atomic to micron scales

Large populations of electromagnetic radiation (EMR) pulses occur at low stresses under both uniaxial and triaxial loadings of chalk samples, in association with the pore deformation (Fig. 3) within the rock⁴⁰ (Bahat *et al.* 2001). Since EMR pulses are created solely by cracks and not by existing defects, this deformation must be linked with cracking in the micron scale⁴¹ (Rabinovitch *et al.* 2003). This interpretation rests on our new model of EMR inducement by *charge oscillations along a propagating crack*³⁹ (Fig. 4). According to this model a line of bonds is located at the front (tip) of the propagating crack. The **bonds break** when the front moves to the next line. The atoms on both sides of the bonds are moved to ‘non equilibrium’ **positions** in relation to their steady state **and perform oscillations around them, at the new surfaces, which give rise to EMR**. The **positive charges** on these surfaces move **together** in one direction away from the equilibrium plane (one crack side), while the **negative charges** move in unison in the other direction from the equilibrium plane (the same crack side), and vice versa, retaining an overall charge neutrality throughout. These surface oscillations, similar to Rayleigh waves, decay exponentially into the bulk.

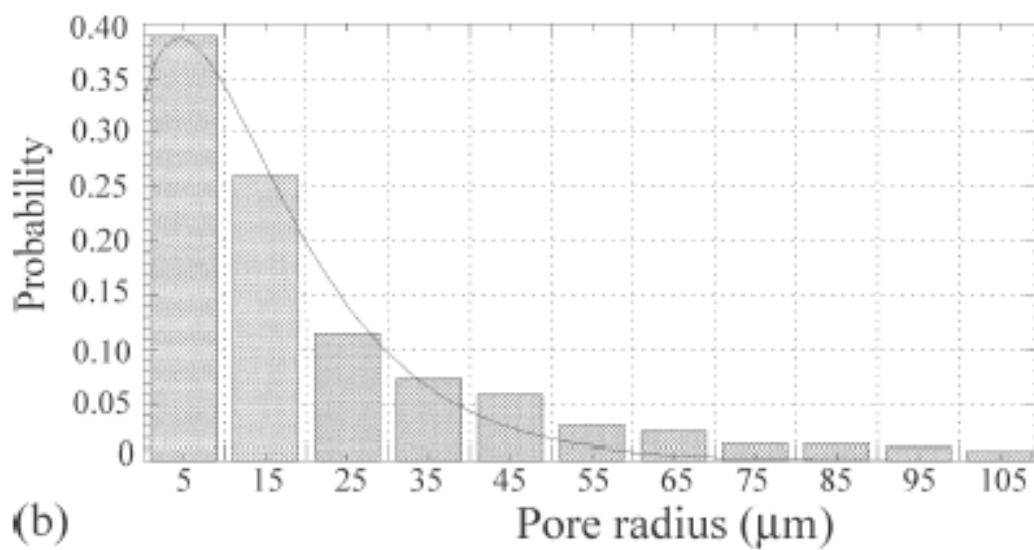
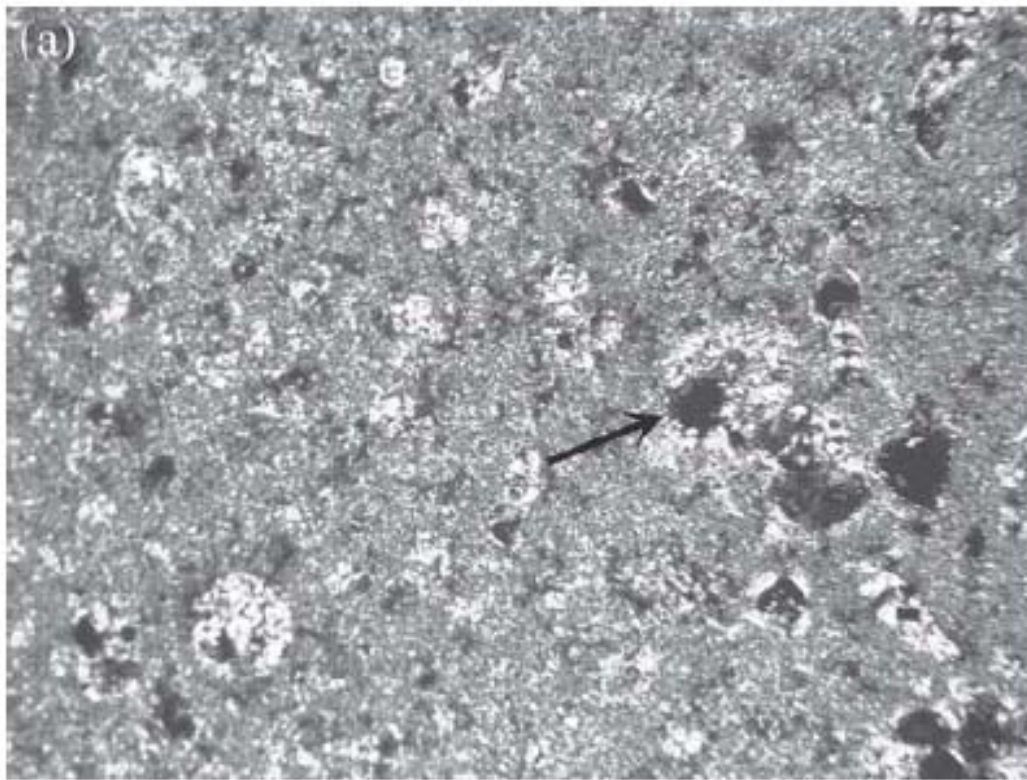


Fig. 3a Photomicrograph of a Middle Eocene (Horsha Formation) chalk (width of picture is 1.2 mm). *Large white spots* are plankton skeletons, *small white spots* are microsparites, and *gray patches* are micrites (calcite). *Black spots* are pores (the one shown by *arrow* is 84 μm in diameter) and iron oxide grains. **b** Measured pore radii distribution in **a**, fitted to $P'(r) = a^2 r \exp(-ar)$; best fit obtained for $a = 0.105 \pm 0.004 \mu\text{m}^{-1}$ ($R^2 = 0.98$) (**a** and **b** after [Rabinovitch et al. 2003a](#))

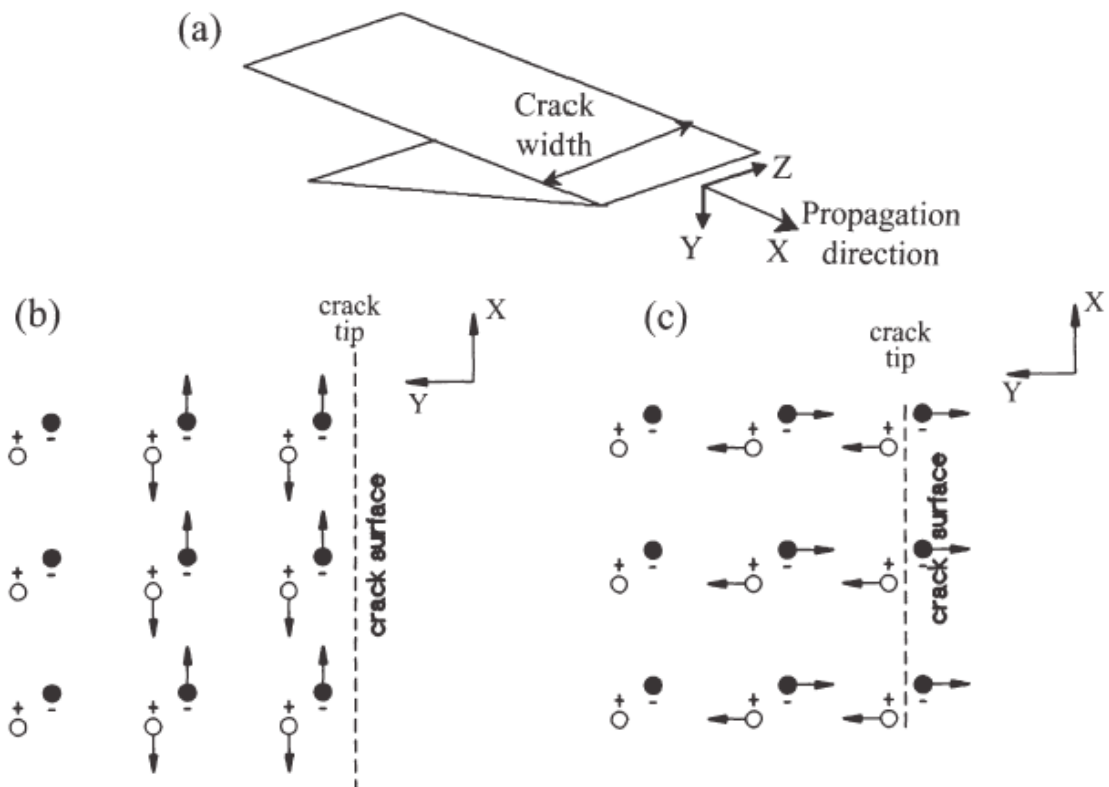


Fig. 4 a A schematic picture of crack propagation; **b, c** schematic “optical surface wave” at crack surface (a similar wave propagates on the other surface) at a specific time. Crack surface is in the xz - plane and the crack moves in the x -direction. Note that charge separation can either be longitudinal (**b**) or transverse (**c**) with respect to the surface, with appropriate EMR polarizations. Note also the exponential decay of the wave into the material. Charge separation is oscillatory so that at a later time the dipole directions are reversed (from Frid et al. 2003)

Fractography in various scales

The basic fractographic elements of the fracture surface (also termed fracture surface morphology) are maintained through various orders of magnitude, from micron sizes, in fractured fibers in metal/glass-ceramic composites⁴² ([4] to tens of meters sizes, in geological exposures (Fig. 5). Furthermore, the fracture stress that induces fracturing may be calculated in all these scales, because this process obeys the same rules of fracture-mechanics. This was used successfully for ceramics and glass^{4,5} () as well as for metals⁴³ (). Geologically, it enables to estimate fracture-paleostresses (that were effective millions of years ago⁴⁴, Bahat and Rabinovitch 19) (Fig.5).

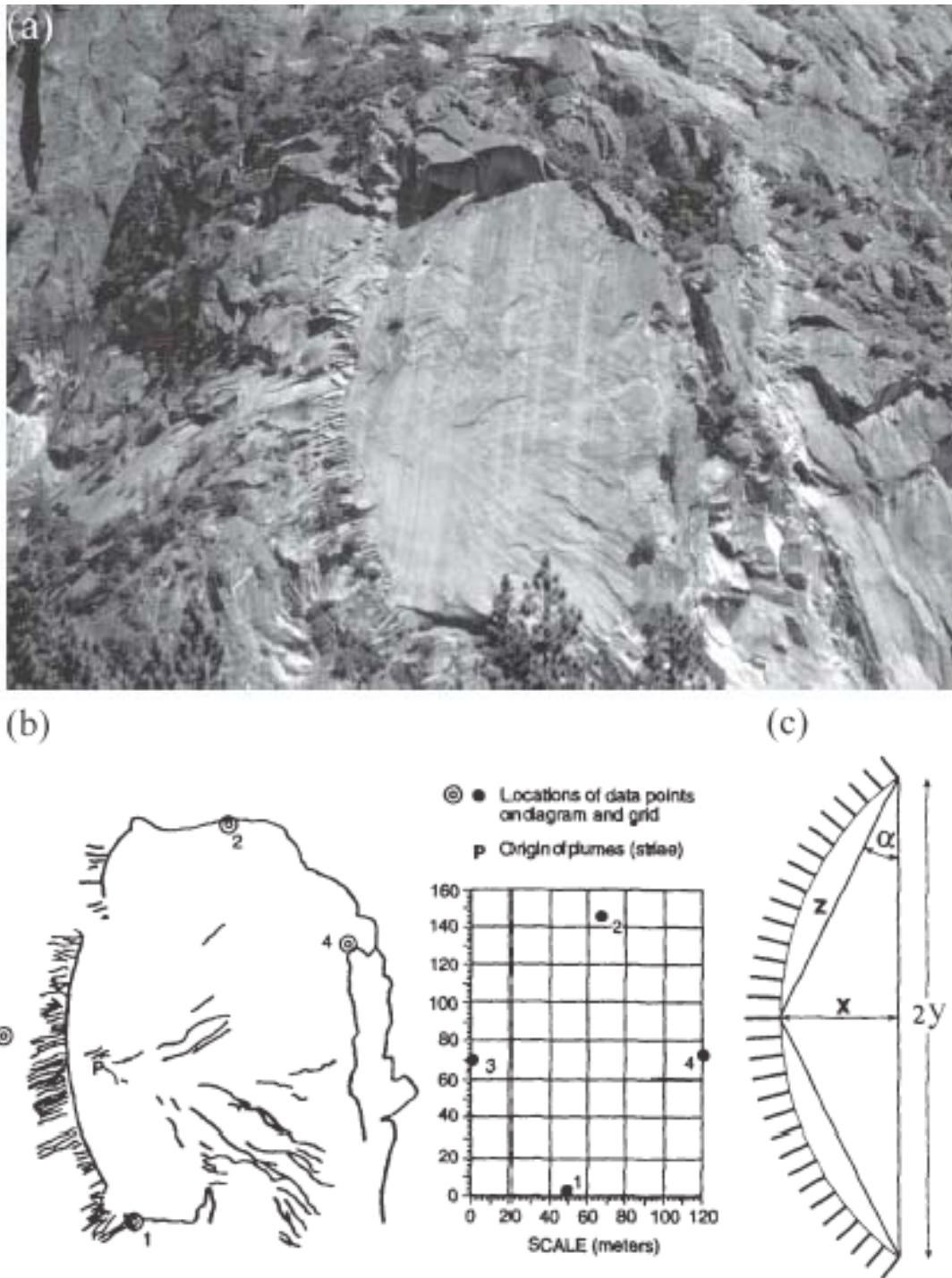


Fig. 5 The calculation of mirror radius when it is unmeasurable on the outcrop, applied on exfoliation joints striking N 27° E and dipping 42° NW on the southwestern side of Half Dome at Yosemite National Park. **a** Photograph of a curved fringe of *en echelon* cracks at left representing a remnant of an exfoliation joint (whose origin has been at the right side of the outcrop) on a slice that has

been removed. **b** Scaled diagram and grid of **a**. The removal of the external slice exposed the surface of a second exfoliation joint whose origin is identified at P by the meeting area of radial barbs of a large plume. **c** Diagram showing the curved inner boundary of the fringe of *en echelon* cracks and the angle \bullet between $2y$ and z (from Bahat et al. 1999) **MORRRRRE**

Tensile fracture versus shear fracture in the mm-cm scale

A full understanding of developments in fracture geology is often hampered by our limited ability to distinguish between “pure” tensile loading (mode I) and processes controlled by shear stresses and mixed mode loading (of modes I, II and III in different combinations), particularly in small sizes (mm-cm). We developed a fractographic technique that enables the distinction of tensile from shear fracture surfaces in laboratory investigation of chalk⁴⁰ (Fig. 6 [2, Fig. 2.16]). This technique has been used successfully in studying a series of problems⁴⁵.

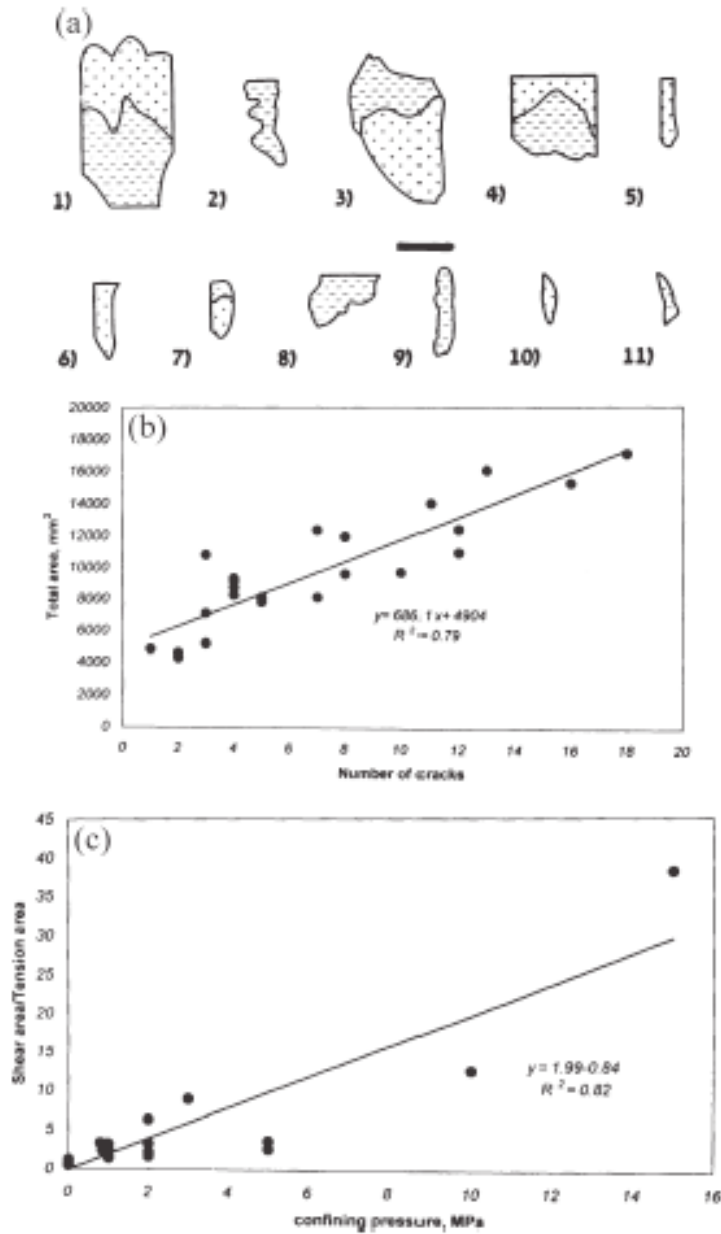


Fig. 6a A display of half of the total number of fracture surfaces (one of each matching couple) from a sample. Shear surfaces are marked by ‘-’ and tensile surfaces by ‘+’. *Scale bar* is 4 cm. **b** Relationship between the number of fractures (one from each two matching fractures) and total area of all fractures. **c** Relationship between the ratio of (fractured area by shear) / (fractured area by extension), and lateral compression, •3 (from Bahat et al. 2001a)

Fractography of fracture in granites in the meter to tens of meters scale

Tensile fractures in rocks, that are termed ‘joints’ by structural geologists, which occur in granites, reveal fracture surfaces meters in size in the Mrákotín quarry from the Czech republic. These surfaces consist of mirror planes and hackle fringes which imply dynamic (rapid) fracture that took place during the cooling stage of the rock, at some 10 km depth (Fig. 7)⁴⁶. [2, Fig. 4.11] (Bahat et al. 2003).



Fig. 7 Joints in the Mrákotín quarry. Photograph of the 025° trending joint A. *Vertical ruler* is 2 m (from Bahat et al. 2001c)

Mapping paleostresses and their rotation with time in km scales.

Measurements of joint directions in many outcrops can provide geological maps of paleostress trajectories. This is based on the theory that the stress trajectories of the maximum horizontal principal stress parallels the strain directions recorded by the joints, along stretches of tens of km long^{22(Sect.6.3)}.

References

- [1] Ravi-Chandar K, Knauss W (1999) Processes controlling fast fracture of brittle solids. *Comput Sci Eng* 1999 Sept/Oct:24–31.

- [2] Bahat D., Rabinovitch A and Frid V. (2004) Tensile fracturing in rocks. Springer-Verlag, Heidelberg (in press).
- [3] Frid V, Rabinovitch A, Bahat D (2003) Fracture induced electromagnetic radiation. *J Phys D Appl Phys* 36:1620–1628.
- [4] Stewart RL, Chyung K, Taylor MP, Cooper RF (1986) Fracture of Sifiber/glass -ceramic composites as a function of temperature. In: *Fracture mechanics of Ceramics*. Plenum Press 7: 33-51
- [5] Bahat D (1991) *Tectonofractography*. Springer-Verlag, Heidelberg.